NO. 45

Selective Defects Synchronize Thermoelectric Performance of $V_{0.9}Fe_{0.5}Co_{0.5}Sb$-based Half-Heusler

Yuzuru Miyazaki[1*], Xue Nan[1], Kei Hayashi[1], Chen Chen[2], Md All Amin Newton[2], Hezhang Li[2, 3], Jing-Feng Li[1, 2]

[1]Department of Applied Physics, Graduate School of Engineering, Tohoku University, Sendai 980-8579, Japan
[2]State Key Laboratory of New Ceramic Materials, School of Materials Science and Engineering, Tsinghua University, Beijing 100084, People's Republic of China
[3]Department of Precision Instrument, Tsinghua University, Beijing 100084, People's Republic of China
* E-mail: yuzuru.miyazaki.b7@tohoku.ac.jp

Introduction

Half-Heusler compounds (HHs) [1]

- ✓ Promising mid-to-high temperature thermoelectrics.
- ✓ Excellent electrical transport, but high thermal conductivity.

Challenges of *XYZ* HHs

- ✓ Decoupling electrical and thermal transport [2].
- ✓ Complex intrinsic defects: vacancies X_v and interstitials Y_i, etc [3].
- ✓ Unclear roles of defect-complex HHs in thermoelectric transport.

Purpose

Design 18-electron defect-complex HHs to *synergistically optimize electrical and thermal transport*.

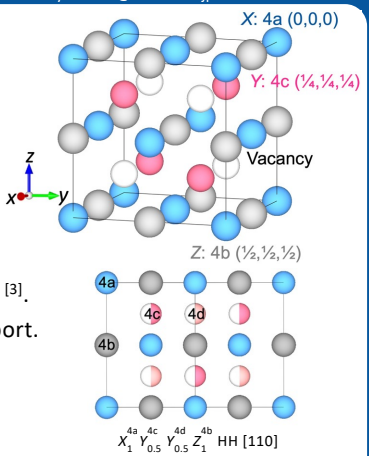


Figure 1. The crystal structure of HH structure with the zoom-in on structural projection along [110] direction.

Methodology

$V_{0.9}Fe_{0.5+x}Co_{0.5-x}Sb$ **HH compounds**

Preparation

- Arc-melting 3 times, in Argon
- Spark plasma sintering, under Vacuum
- Annealing, under Vacuum

Characterization

- Powder X-ray diffraction (XRD)
- Scanning transmission electron microscope (STEM)
- Electron backscatter diffraction (EBSD)
- Scanning electron microscope (SEM)

Measurement

- Electronic properties: σ, S, PF
- Thermal conductivity: κ_{ele}, κ_{lat} and κ_{tot}

Results and Discussion

Atomic-Scale Defect Configuration

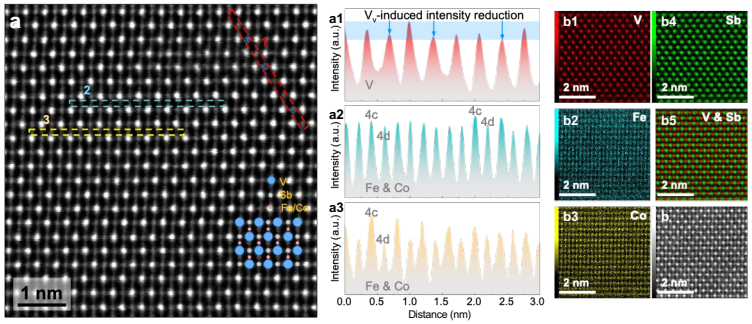


Figure 2. (**a**) The atomic-resolution HAADF-STEM image of $V_{0.9}Fe_{0.5}Co_{0.5}Sb$ lattice along [110] direction. The intensity profiles of a1, V atom at 4a site; **a2**, **a3**, Fe and Co atoms at 4c and 4d sites, corresponding to the dashed rectangle in (**a**) are depicted with the same color. The intensity contrast at 4c and 4d sites suggests random occupation with Fe and Co chemical disorder in (**b2** and **b3**). According to (**b**) the atomic-scale EDS mapping, the corresponding elemental distributions of **b1**, V, **b2**, Fe, **b3**, Co, **b4**, Sb and **b5**, overlapped V & Sb are scanned at the atomic-column level.

- Nano-scale observation on V_v and 4c & 4d site occupancy.
- Atomic-resolved observation on randomly distributed Fe & Co on both 4c and 4d site.

Defect-Induced Microstructure Refinement

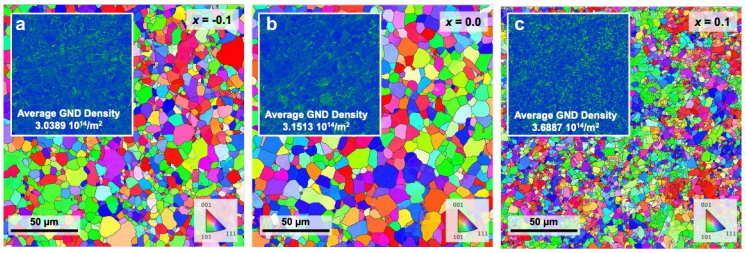


Figure 3. Electron backscatter diffraction (EBSD) crystal-orientation maps of $V_{0.9}Fe_{0.5+x}Co_{0.5-x}Sb$ samples, (**a**) x = -0.1, (**b**) x = 0 and (**c**) x = 0.1 samples, with the corresponding geometrically necessary dislocation (GND) density maps as inserted.

- Fe enrichment induces pronounced grain refinement and increases the density of internal grain boundaries.
- The simultaneously increased GND density indicates enhanced lattice distortion and defect complexity, providing additional phonon-scattering centers.

Enhanced Electrical Transport

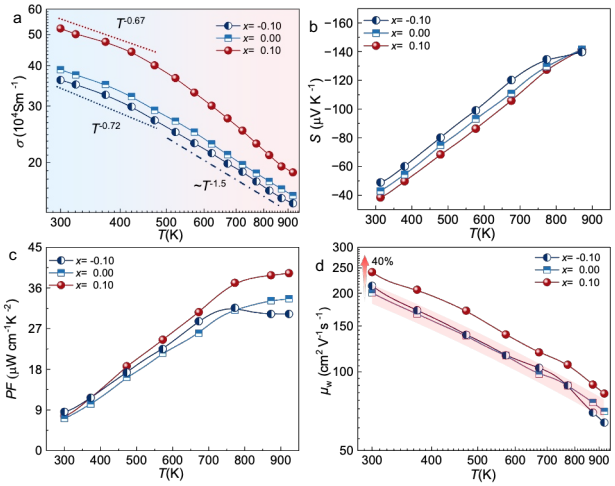


Figure 4. Temperature-dependent (**a**) electrical conductivity, (**b**) Seebeck coefficient, (**c**) power factor and (**d**) weighted mobility of $V_{0.9}Fe_{0.5+x}Co_{0.5-x}Sb$ HH samples.

- Fe enrichment markedly enhances electrical transport, yielding higher electrical conductivity, weighted mobility, and power factor.

Suppressed Lattice Thermal Transport

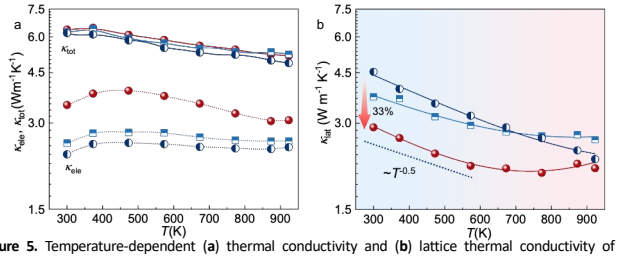
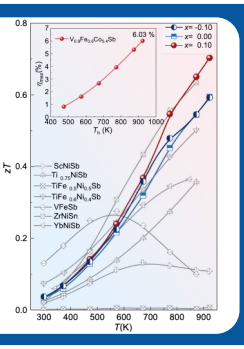


Figure 5. Temperature-dependent (**a**) thermal conductivity and (**b**) lattice thermal conductivity of the $V_{0.9}Fe_{0.5+x}Co_{0.5-x}Sb$ HH samples.

- κ_{lat} is reduced by ~33%, indicating substantially enhanced phonon scattering.

Conclusions

- ✓ Intrinsic defects, including V_v and interstitial Fe_i and Co_i.
- ✓ Fe enrichment → enhanced σ, μ_w and PF.
- ✓ Lattice distortion & grain refinement → around 33% lower κ_{lat}.
- ✓ The synchronized electrical and thermal transport leads to superior thermoelectric performance, with a maximum zT of ~ 0.7 at 973 K.



References

[1] W. G. Zeier *et al.*, *Nat. Rev. Mater.* 2016, **1**(6), 16032.
[2] H. Shen *et al.*, *Nat. Phys.* 2023, **19**(11), 1649-1657.
[3] L. Hu *et al.*, *npj Comput. Mater.* 2025, **11**(104).

Acknowledgements

This work was partly supported by the Grant-in-Aid for scientific research from the Japan Society for the Promotion of Science (No. 23H00230), Tsinghua University Initiative Scientific Research Program via Tsinghua-Tohoku Collaborative Research Fund, and JST SPRING from the Japan Science and Technology Agency (No. JPMJSP2114).